NMR Studies of the Structure and Interactions of Block Copolymer Micelles in Water. 4. Diffusion of Organic Solubilizates into the Micellar Core

J. Kříž,* B. Masař, and D. Doskočilová

Institute of Macromolecular Chemistry, Academy of Sciences of the Czech Republic, 162 06 Prague 6, Czech Republic

Received November 19, 1996[⊗]

ABSTRACT: Solubilization of relatively hydrophobic organic compounds (solubilizates) by the core of poly(methyl methacrylate)-*block*-poly(acrylic acid) (PMMA−PAAc) micelles in D_2O was theoretically simulated and experimentally studied for a number of compounds such as chloroform, chlorobenzene, 4-methylcyclohexanone, benzene, toluene, cyclohexane, and hexane. The experimental results show that (i) the core-captured amount of the solubilizate as well as its solubilization rate chiefly depend on its interaction with PMMA (expressed, e.g., by its χ-parameter), (ii) the limiting solubilization degree may also be determined by other thermodynamic factors, in particular the core−water interphase tension, (iii) the solubilization rate and partly the equilibrium solubilization degree are also influenced by shell−core interactions, (iv) most solubilizates, except chloroform, swell the core with a surprisingly narrow front, which could indicate a steep concentration dependence of their diffusion coefficient but also (v) there is morphological inhomogeneity of the core with more easily accessible domains in the outer part of the core. The last conclusion is also supported by the much lower solubilization rates observed with micelles formed by copolymers with longer PMMA blocks.

Introduction

In our previous studies,[1−3] nuclear magnetic resonance was shown to offer interesting results concerning the structure, dynamics and various interactions of poly(methyl methacrylate)-*block*-poly(acrylic acid) (PMMA−PAAc) micelles in water or D_2O. Most of these results concerned the mobility of the micellar shell[2] or its interaction with organic solubilizates.[3] However, the most interesting interactions, theoretically as well as practically, are those of the micellar core with organic substances, i.e., the solubilization process as such.[4−7] Although quite simple in principle, this process turns out to be quite complicated in real systems. Therefore, we deal with it in the present separate study.

Theory

In this study, we are dealing not only with structural and equilibrium phenomena but also with kinetic aspects. The experimental arrangement—which is dictated by the used method, namely NMR, and by the nature of the system under observation, a very dilute dispersion of micelles that are many orders of magnitude smaller than the distance between the starting point of diffusion and the area of observation—is apparently not very suitable for kinetic studies. To see to what extent our results can be at least semiquantitatively relevant from the point of view of solubilization dynamics, we have to simulate the processes under observation. This is the content of the present part.

To be able to simulate our experimental results, we have to build a mathematical model describing in a sufficiently realistic way the diffusion of a very slightly water-soluble organic substance through water into the micellar cores. Our system consists of two superimposed cylindrical layers, usually the upper one (column 1) formed by the neat organic substance that is going to be solubilized by the micelles and the lower one (column 2) by a micellar solution of the block copolymer in water. Column 2 is placed to be axially symmetrical with respect to the plane of the NMR receiving coil. The upper layer contains enough substance to ascertain a constant concentration gradient at the interface.

The basic physical process that our model has to describe is the diffusion of the organic substance (called solubilizate in the further discussion) into its water solution, through water and the micellar shell into the shell−core interface, and gradually into deeper core layers. In spite of eventual differences in chemical shifts, it is generally impossible to discriminate by NMR between the solubilizate dissolved in water and that penetrated into different layers of the micellar core because of their relatively rapid exchange. Our final task is thus to simulate the time evolution of the cumulative concentration of the solubilizate in a thin cylindrical layer radially bisected by the plane of the receiving coil.

To make the mathematical model feasible, we are forced to accept a number of approximations. The following list is sufficient to make the calculations practicable without impairing seriously their physical meaning.

A1: The micelles are sufficiently small in comparison with the length of column 2 so that each of them can, with its local radial surroundings, be considered as a point x of the longitudinal dimension of the system.

A2: The micelles are sufficiently distant from each other so that they do not mutually influence the concentration gradient of the solubilizate in the vicinity.

Consistently with A1 and A2, the local vicinity of a micelle, and thus of a point x, can be considered as radially symmetrical. As the radial distance from the center of the core, in which there is a significant concentration gradient, must be very small in comparison with the radius of the column, we propose to neglect it in first approximation. This leads to the following approximations.

A3: The concentration gradient of the solubilizate in any direction perpendicular to x is vanishing, and the

[⊗] Abstract published in *Advance ACS Abstracts,* June 15, 1997.

S0024-9297(96)01701-9 CCC: $14.00

diffusion through water can thus be solved in one dimension x only.

A4: The solubilizate is the only species diffusing through water in the dimension x with the diffusion coefficient D_W; i.e., the complementary diffusion of micelles can be neglected due to their much larger volume.

In addition to these approximations, we take the following physically justified assumptions.

AS1: The radial diffusion through the water−micelle interface (in particular water−core interface) is of the kind of extraction characterized by the partition coefficient $\xi \gg 1$. We assume that ξ does not depend on the amount S_C of the solubilizate in the core.

AS2: The diffusion coefficient of the radial migration of the solubilizate between individual layers of the micellar core D_M generally depends on its concentration, i.e., $D_M(\rho) = f(C)$.

AS3: The volume of the micellar core grows with the amount of the solubilizate swollen into it. In the absence of specific solubilizate interactions with the core polymer, the core volume $V_C = V_{C0} + S_C h$, where h is the density of the solubilizate and V_{C0} is the original core volume.

There is a critical value V_C^{crit} given by the thermodynamics of the system that the core volume cannot surpass. The question whether ξ should take care of maintaining V_C within its bounds depends on the definition of ξ. Although it seems to be more natural to connect the value of ξ with the type of the core polymer rather than with the thermodynamics of the micellar system expressed by the value of V_c^{crit}, the lack of knowledge of the right dependence of ξ on V_C forces us to take another approximation, viz: A5: ξ is independent of the swelling of the core by the solubilizate and is defined by the relation $\xi = C_M(\infty)/C_W(\infty)$, where $C_M(\infty)$ and $C_W(\infty)$ are the respective equilibrium concentrations of the solubilizate in the micellar core and in the surrounding water.

With the approximations A1−A5 and the assumptions AS1−AS3, the mathematical model of our system can be expressed in the following difference form:

$$C_W(x+\Delta x,t+\Delta t) = C_W(x+\Delta x,t) + j_x(t)\Delta t/\pi r^2\Delta x - j_e(x,t)\, p(\rho_C,\rho_C+\Delta\rho)\Delta t/\{4/3\pi[(\rho+\Delta\rho)^3 - \rho^3]\} \quad (1)$$

$$C_M(x,\rho+\Delta\rho,t+\Delta t) = C_M(x,\rho+\Delta\rho,t) + [j_e(x,t) - j_m(x,\rho,t)]\Delta t/\{4/3\pi[(\rho+\Delta\rho)^3 - \rho^3]\} \quad (2)$$

$$C_C(x,\rho,t+\Delta t) = C_C(x,\rho,t) + j_m(x,\rho-\Delta\rho,t)\Delta t/\{4/3\pi[\rho^3 - (\rho-\Delta\rho)^3]\} \quad (3)$$

where $C_W(x,t)$, $C_M(x,\rho+\Delta\rho,t)$, and $C_C(x,\rho,t)$ are the solubilizate concentrations in water, in the surface core layer, and in the core layer with radius in the range from ρ to $\rho - \Delta\rho$, respectively. The expressions of the diffusion flows used in eqs 1−3 are

$$j_x(x,t) = D_W\pi r^2[C_W(x-\Delta x,t) - 2C_W(x,t) + C_W(x+\Delta x,t)]/\Delta x \quad (4)$$

$$j_e(x,t) = D_C 4\pi\rho_C^2[C_W(x,t) - C_C(x,\rho_C,t)/\xi]/\Delta\rho \quad (5)$$

$$j_m(x,\rho,t) = D_C 4\pi\rho^2[C_C(x,\rho+\Delta\rho,t) - 2C_C(x,\rho,t) + C_C(x,\rho-\Delta\rho,t)]/\Delta\rho \quad (6)$$

where D_W and D_C are the solubilizate diffusion coefficients in water and the core, respectively, D_C being a function of solubilizate concentration $D_C(C)$ to be defined later on. The probability $p(\rho_C,\rho_C+\Delta\rho)$ of the given point being in a surface area of a micellar core with the radius ρ_C used in eq 1 is

$$p(\rho_C,\rho_C+\Delta\rho) = \varphi(t)\{1 - [\rho_C/(\rho_C+\Delta\rho)]^3\} \quad (7)$$

where φ(t) is the time dependent volume fraction of the micellar cores in the system. The volume of the micellar layer between ρ and $\rho + \Delta\rho$ expands in the following way:

$$V_C(x,\rho,t+\Delta t) = V_C(x,\rho,t)\{1 + [C_C(x,\rho,t+\Delta t) - C_C(x,\rho,t)]/h\} \quad (8)$$

and its radius ρ changes accordingly with the third root.

For the concentration dependence $D_C = D_C(C)$, we assume for our purpose the reasonably convergent formula

$$D_C = D_C(0) + D_C(\infty)[1 - \exp(-\alpha C_C)] \quad (9)$$

where C_C is the solubilizate concentration in the core and $D_C(0)$ and $D_C(\infty)$ are its diffusion coefficients in the intact and fully swollen core polymer, respectively.

From the form of eqs 1−9, it is clear that the whole system is interdependent and cannot be but numerically solved. The following simulations were done using a procedure based on the above equations.

Figures 1−3 show simulated time dependences of $C = (1 - \varphi_M - \varphi_C)C_W + \varphi_M C_M + \varphi_C C_C$, φ_M and φ_C being the volume fractions of the shell−core interface and core areas, which in all cases are assumed to be 1.0×10^{-4} and 9.0×10^{-4}, respectively. The core radius ρ_C in all cases is 40 nm, the remaining variables being $D_W = 1.0 \times 10^{-5}$, $D_C = 0.2 \times 10^{-5}$ cm^2 s^{-1}, and the partition coefficient $\xi = 2.0 \times 10^3$ if not stated otherwise

Figure 1 shows $C(t)$ in water (1) and in micellar solutions with $D_C = 2.0 \times 10^{-6}$ (2), 4.0×10^{-6} (3), and 6.0×10^{-6} (4) cm^2 s^{-1}, ξ being the same in cases 2−4. Figure 2 gives simulations with the same D_C but $\xi = 2.0 \times 10^3$ (1), 3.0×10^3 (2), and 4.0×10^3 (3). From the comparison of both figures, one can see that a higher diffusion coefficient and higher partition coefficient (or solubilization capacity) of the core have a similar but not quite analogous effect on $C(t)$. This distinction is important because D_C depends mainly on the molecular size whereas ξ is chiefly associated with the Flory−Huggins χ parameter of the solubilizate. As the value of ξ, or some main value of it, can be obtained from the equilibrium $C(\infty)$, one can, in a semiquantitative way at least, extract information about solubilization kinetics from the experimental curve.

In both Figures 1 and 2, D_C was assumed to be constant, i.e., $\alpha = 0$ in eq 9. Figure 3 shows a serious complication, giving $C(t)$ for $\alpha = 0.0$ (1), 0.5 (2), 1.0 (3), and 1.5 (4). Growing D_C with C_C can thus, to some degree, mimick faster initial solubilization. As seen when comparing Figures 3 and 1, the effect is not quite the same, however. In addition to it, steeper $D_C(C)$ dependences can be expected in the case of higher χ, i.e., higher ξ and differentiated that way. There appears to be an additional interesting effect of a steep $D_C(C)$

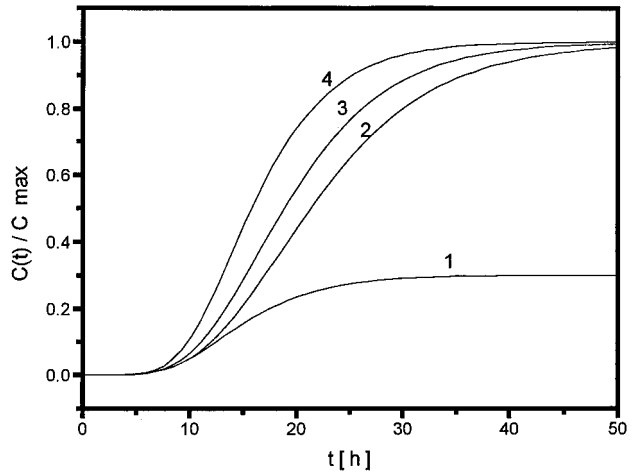

Figure 1. Simulations of $C(t)$ in water with $D_W = 1.0 \times 10^{-4}$ cm^2 s^{-1} (1) and in micellar solutions with $D_C = 0.2 \times 10^{-4}$ (2), 0.4×10^{-4} (3), and 0.6×10^{-4} (4) cm^2 s^{-1}, $\xi = 10^3$.

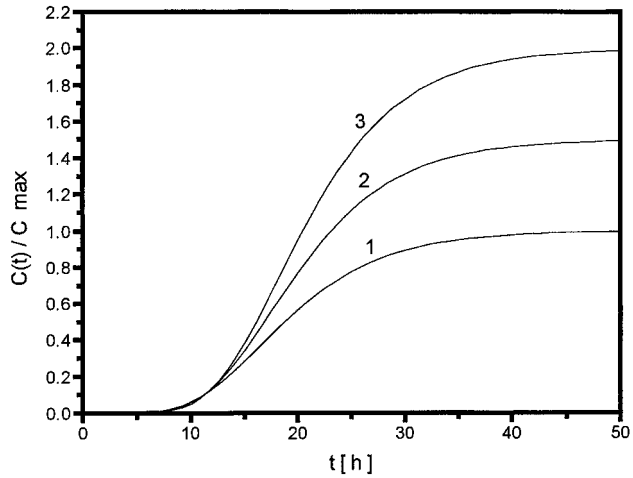

Figure 2. Simulations of $C(t)$ with $D_C = 0.4 \times 10^{-4}$ cm^2 s^{-1} and $\xi = 2.0 \times 10^3$ (1), 3.0×10^3 (2), and 4.0×10^3 (3).

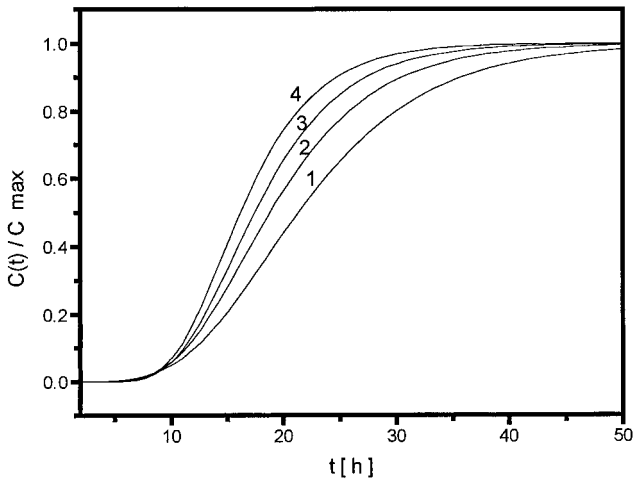

Figure 3. Simulations of $C(t)$ with $D_C(0) = 0.2 \times 10^{-4}$ and $D_C(\infty) = 1.0 \times 10^{-4}$ cm^2 s^{-1} for $\alpha = 0.0$ (1), 0.5 (2), 1.0 (3), and 1.5 (4).

dependence illustrated by Figure 4a,b, which show the development of the radial concentration profile of the solubilizate with increasing total solubilized amount (given as the percentage of the maximum amount).

The following general conclusions can be drawn from these simulations: (i) the experimental $C(t)$ curve reflects the dynamics of solubilization (its onset and

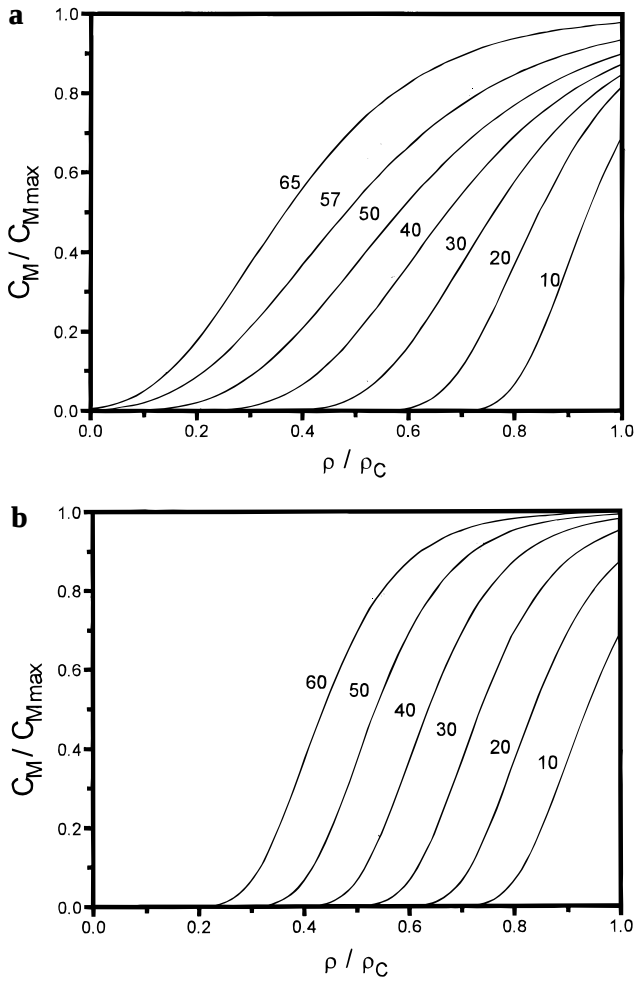

Figure 4. (a) Simulations of $C_C(\rho)$ for $\alpha = 0$, the remaining constants as in Figure 3, for the indicated degrees of core swelling ($C_C(\infty)$ for all ρ being 1.0). (b) Same as Figure 4a, $\alpha = 2.0$.

main slope can be considered as a semiquantitative measure of its kinetics whenever the cases with the same ξ or χ parameter are compared); (ii) in the interpretation of the experimental $C(t)$ dependences, however, possible effects of higher ξ or α have to be considered.

Experimental Section

Chemicals. Poly(methyl methacrylate)-*block*-poly(acrylic acid) copolymers (PMMA−PAAc) were prepared from the corresponding poly(methyl methacrylate)-*block*-poly(*tert*-butyl acrylates) by the methods described earlier.[1−3] The 0.5% w/w D_2O micellar solutions of PMMA−PAAc were mostly prepared by direct dissolving of the copolymer freeze-dried from its H_2O solution. In the cases where such procedure was not feasible, H_2O or H_2O−LiCl micellar solutions were converted into D_2O solutions by dialysis.

NMR Measurements. ^{1}H NMR spectra were measured with Bruker ACF 300 and Bruker Avance DPX 300 spectrometers using the methods fully described in previous papers.[1−3]

Results and Discussion

Most of the results reported here were obtained with PMMA−PAAc (or their alkaline salts) of moderate molecular weight (the respective mean polymerization degrees of the PMMA and PAAc blocks being 92−93 and 149−275) and not quite narrow molecular weight distribution (its polydispersity ranging from 1.1 to 1.8). Such block copolymers, if transferred to water from their

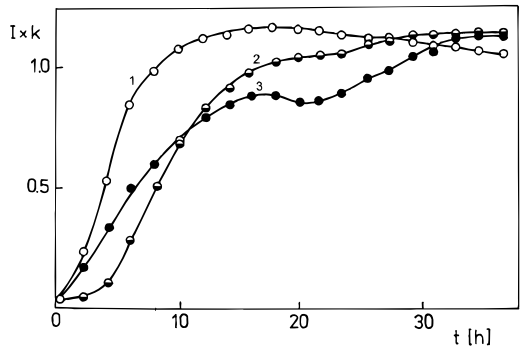

Figure 5. Experimental solubilization curves for the system D_2O, PMMA−PAAc, chloroform at 333 K. Signal intensity of (1) chloroform, (2) PMMA−OCH_3, and (3) PAAc α-CH (intensity increase).

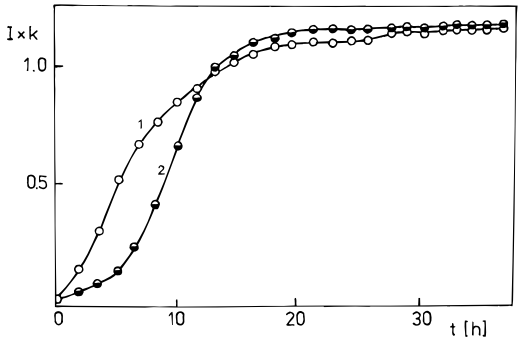

Figure 6. Experimental solubilization curves for the system D_2O, PMMA−PAAc, 4-methylcyclohexanone (MC) at 333 K. Signal intensity of (1) MC, and (2) PMMA −OCH_3.

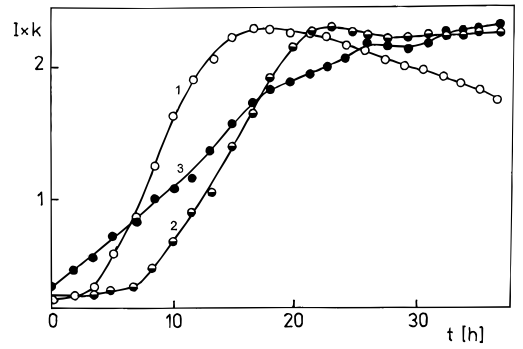

Figure 7. Experimental solubilization curves for the system D_2O, PMMA−PAAc, benzene at 333 K. Signal intensity of (1) benzene, (2) PMMA −OCH_3, and (3) PAAc α-CH (intensity increase).

tetrahydrofuran−water solution by dialysis and freeze-dried, can be directly dissolved in D_2O forming medium-sized micelles of surprisingly narrow size distribution[1] that are able to solubilize organic substances in a wide range of their PMMA-related χ parameters. Copolymers with longer blocks, in particular those of PMMA, behave differently and will be dealt with separately.

Solubilization Rate and Capacity Related to the χ Parameter. Figures 5−7 illustrate the relatively early stages of the solubilization experiments with the same 0.5% w/w micellar solutions of PMMA−PAAc and chloroform, 4-methylcyclohexanone, and benzene, respectively. With different scales, Figures 5−7 contain integral signal intensities of the solubilizate (the methyl signal in the case of 4-methylcyclohexanone) and of the −OCH_3 protons in the PMMA block and, where possible, the relative signal intensity increase of the PAAc α-CH signals. In Figure 8, which will be discussed later, one of the curves (1) corresponds to the analogous time dependence of the chlorobenzene signal.

Comparing these figures with the simulations in the Theory one can see that the solubilization rate decreases in the order chloroform > chlorobenzene > methylcyclohexanone > benzene > toluene (the last one not being illustrated). Table 1 compares the extreme slopes κ of the solubilization curves with the total amount of the solubilized substance (corrected for its solubility in D_2O and relative to the core mass) and its χ parameter with PMMA. Although there are differences in the water-related diffusion coefficients and solubilities that influence the slope of the solubilization curve, one can conclude that the solubilization proceeds not only to a higher extent but also more readily with solubilizates that are better solvents for PMMA.

This result, already foreseen in one of our earlier papers,[1] can be supplemented with a more detailed insight into the solubilization process, as shown in the next paragraph.

Table 1 gives also the values of the "apparent partition coefficient" ξ^*, which is simply the ratio of the respective concentrations in the micelle and in the surrounding D_2O (i.e., the corresponding solubility in D_2O) at micelle equilibrium saturation. At this stage, the surrounding D_2O is also saturated with the same substance as assured by the experimental conditions. The value of ξ^*, of course, does not reflect the true ξ, which is practically unattainable in our case, but points to a rather serious question. As can be seen from Table 1, the correlation of equilibrium core concentrations C_C with χ is much better than that of ξ^*. Serious anomalies occur, as expected, in the case of solubilizates that are more soluble in water. In such cases, even true ξ for the case of geometrically unconstrained polymer would be somewhat lower. Nevertheless, the large deviation of ξ^* in the case of chloroform, which is an exceptionally good solvent for PMMA, points to the following conclusion. The surface condition $C_C/C_W \rightarrow \xi$ is probably merely the limiting case of the constraint that stops the solubilizate transport into the core at equilibrium. It should be decisive only in cases of relatively low total amounts of the solubilizate in the core. In all other cases, the decisive condition probably is reaching the *core capacity*, i.e., a value given by the thermodynamical stability of the whole micellar system in water. This value apparently depends not only on the nature and size of the core itself, i.e., on the core−unimer interphase tension, but also *on the state of the micellar shell*, as we are going to show below.

Interaction with the Shell−Core Interface and Penetration of the Core. The signal intensity increase of both PMMA OCH_3 and PAAc α-CH protons reflects the increase in the mobility of the respective groups (cf. refs 1−3). As the correlation time change between the bulk and swollen polymer amounts to several orders of magnitude and the half-width $\Delta\nu_{1/2}$ of the corresponding signals does not change perceptibly during the experiment, one can take the signal increase as a direct measure of the fraction of the respective polymer block freed by swelling. In Figures 5−7, one can see that the OCH_3 signal curve approximately copies, with some lag, that of the solubilizate, as one could expect. In both Figures 5 and 7 (the case of 4-methylcyclohexanone in Figure 6 being excluded because of an overlap of the respective signals), the advance of solubilization is accompanied by an increase of the PAAc α-CH signal, however. In our previous

Table 1. Water Solubilities[a] C_W, Flory−Huggins Parameters[b] for PMMA χ, Diffusion Coefficients[c] D_W of Selected Solubilizates Compared with the Equilibrium Core Concentrations $C_C(\infty)$, Maximum Slopes κ, and Apparent Partition Coefficients ξ^* in Their Solubilization with PMMA−PAAc Micelles[d]

solubilizate	C_W, g/L	χ	$10^5 D_W$, cm^2 s^{-1}	$C_C(\infty)$, % w/w	κ, g L^{-1} h^{-1}	ξ^*
chloroform	7.837	0.34	∼1.3	63.2	1.94	80.6
chlorobenzene	0.391	0.36	∼0.85	47.9	1.43	1225.1
4-methylcyclohexanone	22.2	∼0.46	0.84	44.3	1.32	19.9
benzene	1.732	0.44	1.02	41.8	0.58	241.3
toluene	0.562	0.45	0.85	40.2	0.54	715.3
cyclohexane	0.055	∼0.50	0.84	21.3	0.18	3872.7
hexane	0.013	∼0.51	0.80	20.8	0.09	16000

[a] Partly from ref 8. [b] Cf. refs 9 and 10. [c] From ref 11 or guess. [d] P_n(PMMA) = 93, P_n(PAAc) = 149, 0.5% w/w. PMMA−PAAc in D_2O at 333 K.

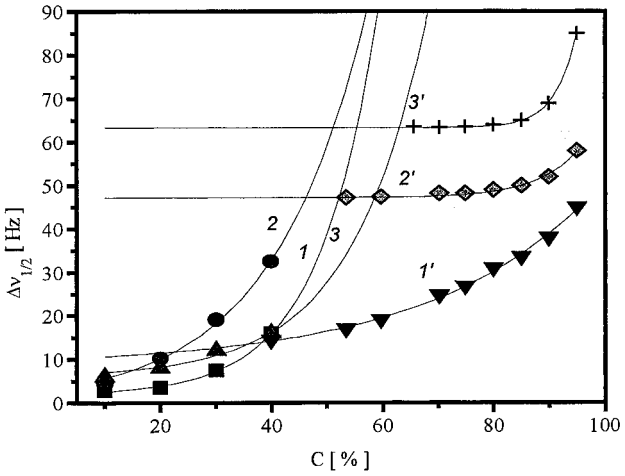

Figure 8. Signal half-widths $\Delta\nu_{1/2}$ of chloroform (1, 1′), chlorobenzene (2, 2′), and benzene (3, 3′) in solutions of PMMA (1, 2, 3) and swollen PMMA core (1′, 2′, 3′) with dependence on the polymer concentration (333 K).

study,[3] we already conjectured this phenomenon to be an effect of the loosening of entwined or entangled PAAc segments near the shell−core interface. Figures 5 and 7 show, however, a monotonous increase of α-CH signals during most of the solubilization process, i.e., even along with the swelling of the core. We have thus to conclude that a substantial part of PAAc segments is entangled with the surface PMMA segments and the shell−core interface is thus much wider and fuzzier than originally thought.

Slightly different information about the diffusion process can be obtained from the half-width $\Delta\nu_{1/2}$ (or $1/T_2^*$) and chemical shift δ of the solubilizate signal. As the exchange between the D_2O-dissolved and core-swollen solubilizate molecules is fast on the NMR time scale,[1] their resonances merge and the chemical shift of the actual signal is a weighted average of those of the isolated sites. Hence the signal shifts with ongoing solubilization. At the same time, the half-width of the signal could be expected to decrease with the growing concentration of the solubilizate, i.e., the less dense state of the core. Figure 8 compares the values of $\Delta\nu_{1/2}$ of three different solvents in the corresponding concentrated solutions of PMMA with those of the same solvents swollen into the micellar core (the range of the compared cases being narrowed on one side by the feasibility of polymer dissolution, on the other by the solubilization capacity of the micelle). In the solubilized state, the half-widths of the signals are partly much lower, partly higher than those expected for the corresponding polymer concentration. Their most apparent feature is, however, their constant value over a wide range of concentration. This phenomenon cannot be explained merely in terms of the signal broadening by exchange because this effect should be not more but less pronounced with higher swelling. Taking into account that (i) the half-width of the PMMA OCH_3 signals is—except in the very early swelling stages—approximately constant, too, whereas (ii) the intensity of the same signal increases, converging to a value generally lower than the theoretical one (which is also found in a true solution of the copolymer, e.g., in pyridine−dimethylformamide 1:1), we have to conclude that notwithstanding the growing total amount of the solubilizate in the core, *its local concentration remains more or less constant; i.e., the frontier of the solubilizate's penetration is rather narrow and apparently stops (or lingers for a very long time) at some non-zero core radius dependent on the nature of the solubilizate.* This can have two principal reasons: (a) the diffusion coefficient of the solubilizate in the core is strongly concentration dependent (i.e., high α, as shown in the Theory) and/or (b) the core is not quite homogeneous but structured with domains more easily accessible to the solubilizate. We find both reasons to be probable, the second and less evident (b) being supported by much slower penetration of the same solubilizates into the depth of the micellar cores formed by several times longer PMMA blocks. These quite recent observations made in our laboratory suggest that, apart from the shell−core interface where segments of different blocks are intermingled, there should exist a *next-to-core surface area composed mostly of the core segments but less densely organized due to interactions with the interface.* In the case of relatively short PMMA blocks, such an area could encompass a substantial part of the core. With several times longer PMMA blocks, however, most of the micellar core would be formed by a dense PMMA polymer reluctant to be swollen even by relatively good solvents. These ideas are strongly supported by our recent observations of high-molecular-weight PMMA−PAAc copolymers. As these results could be complicated by other not quite discerned factors, we shall deal with them in a separate study.

Nonequilibrium Effects: Solubilization of Benzene and Toluene. Most of the solubilization curves such as in Figures 5−7 have a "hump" in their early parts; i.e., they go through a maximum before reaching a somewhat lower equilibrium level. In the same time area, the curves of α-CH as well as OCH_3 signal intensity show various anomalies, usually in the form of a saddle. This phenomenon is more or less general but most apparent with aromatics such as benzene or toluene.

As an example, Figure 9 compares the time dependence of the toluene methyl signal intensity (1, without a scale) with that of its $1/\Delta\nu_{1/2}$ (2) and chemical shift δ (3). The corresponding curves of the signals of aromatic protons of toluene and benzene are quite analogous. In

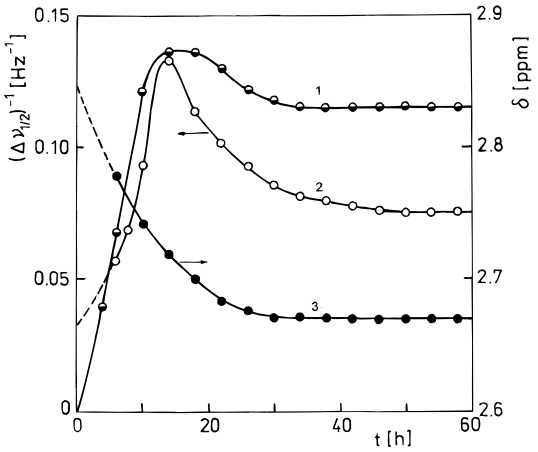

Figure 9. Time dependence of the toluene methyl signal intensity (1, without a scale), its inverse half-width $1/\Delta\nu_{1/2}$ (2), and chemical shift δ (3).

the area of the "hump" of the solubilization curve, T_2* (or $1/\Delta\nu_{1/2}$) clearly goes through a sharp maximum whereas the chemical shift changes continuously. The maximum is less sharp but quite apparent for the aromatic protons, the other features being quite analogous.

The increase in T_2* (or $1/\Delta\nu_{1/2}$) of the solubilizate signal may be caused by two different changes of its dynamics: (i) faster exchange between the water-dissolved and core-bound molecules and (ii) the increased local mobility of the latter. This change is clearly temporal only and subsides as the "excessive" molecules of solubilizate leave the core and the system approaches equilibrium. At the same time, the continuous change in δ of the signal indicates that the majority of the solubilizate molecules enter a state of a closer contact with PMMA segments.

The only plausible explanation of this appears to be some reorganization of the outer core layers in the course of their swelling by the solubilizate. This phenomenon is probably most apparent with aromatic solvents because better, i.e., more polar, solvents exert strong interactions with PMMA segments that mask the effect whereas poor solvents are not able to swell the core and thus loosen its segments effectively.

When accepting this explanation, we have to conclude that even the micelles obtained by direct dissolution of the freeze-dried form of the copolymer are in a *nonequilibrium state.* Recalling that this form was reached by careful dialysis of a true solution of the copolymer with water and the subsequent freeze-drying of the obtained micellar solution, one has to conclude that the nonequilibrium state had to emerge either during the smooth change of the solvent−water gradient in dialysis or during freezing and slow evaporation of the micellar solution. Both alternatives are surprising, but either of them points to a possibility that the nature of the micellar systems is even more subtle than suspected.

Effects of Shell−Core Interactions on the Solubilization Rate. Figure 10 shows curves of chlorobenzene solubilization by equivalent concentrations of PMMA−PAAc, PMMA−PAAcLi, and PMMA−PAAcNa compared with that with pure D_2O. In this case, the polymerization degrees of the PMMA and PAAc (or PAAc salt) blocks were 93 and 149, respectively. The curves indicate that, in the case of such relatively low-molecular-weight copolymer, the early stages of solubilization are faster but the equilibrium solubilized amount is lower with more ionic states of the shell. The

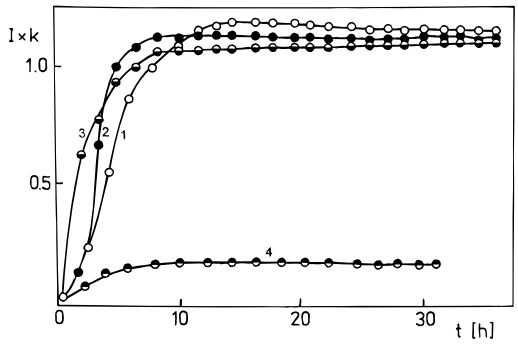

Figure 10. Time dependences of the chlorobenzene signal intensity during its solubilization equivalent concentrations of PMMA−PAAc (1), PMMA−PAAcLi (2), and PMMA−PAAcNa (3) compared with that with pure D_2O (4).

Table 2. Equilibrium Core Concentrations $C_C(\infty)$ and Maximum Slopes κ in Chlorobenzene Solubilization by PMMA−PAAc Micelles in D_2O at 333 K

	P_n			
form	PMMA	PAAc	$C_C(\infty)$, % w/w	κ, g L^{-1} h^{-1}
H	93	149	47.9	1.43
H	92	275	45.4	1.26
H	149	530	37.3[a]	0.61
Na	93	149	45.2	1.69
Na	92	275	43.1	1.06
Na	149	530	28.3[a]	0.48

[a] Obtained by extrapolation.

difference in solubilization rate can be fully explained by the already reported[3] difference in the state of the micellar shell: with growing ionization, the chains are more extended[2] and less entwined[3] so that the approach of the solubilizate molecules to the core is easier. The somewhat surprising difference between the lithium and sodium salts of the PAAc blocks was already stated,[2] too. The unexpected phenomenon observed here is the slight but perceptible tendency of the shell ionization to lower the total solubilized amount. This effect could be associated with the above discussed state of the outer layers of the core, namely by electrostatic dissolution of the core area more easily approachable because of the not very tight embroilment of PMMA and PAAc segments.

This phenomenon reveals its much more complicated, even controversial, nature, however. Table 2 shows the maximum slopes of chlorobenzene solubilization curves and the total solubilized amounts for PMMA−PAAc copolymers with polymerization degrees similar for PMMA but dissimilar for the PAAc blocks. In the case of the longest PAAc, the solubilization is so slow that the equilibrium value has to be determined by extrapolation. In the same table there are also compared the corresponding values for PMMA−PAAcNa. It is easy to see that longer and more ionic blocks of the shell, except the quite short ones, lead to a slower and also lower equilibrium solubilization. The only reasonable cause of this could be a different state of the micellar core in the compared cases.

These findings show that it would be erroneous to consider the state of the micellar core merely from the point of view of the interactions between PMMA blocks themselves and between them as a whole and the surrounding water. Quite clearly, the chains in the shell have not only a stabilizing effect on the micelle as a whole (thanks to their positive interactions with water) but they *also influence the core.* Although the incompatibility of PMMA with water must be the

decisive factor in the formation of a PMMA−PAAc micelle, the *incompatibility of* PMMA *with* PAAc *growing with the chain length and in particular with its ionization reveals itself to be a nonvanishing factor in the subtle energetic balance of the micelle, too.* Such a complication is not very inviting when considered as an obstacle for easy generalizations but could be fruitful for further understanding of supramacromolecular systems.

Acknowledgment. The authors thank the Grant Agency of the Czech Republic for financial support given under Grant No. 203/95/1319.

References and Notes

(1) Kříž, J.; Masař, B.; Pospíšil, H.; Pleštil, J.; Tuzar, Z.; Kiselev, M. A. *Macromolecules* **1996**, *29*, 7853.
(2) Kříž, J.; Masař, B.; Dybal, J.; Doskočilová, D. *Macromolecules* **1997**, *30*, 3302.
(3) Kříž, J.; Masař, B.; Dybal, J. *Macromolecules*, submitted for publication.
(4) Cao, T.; Munk, P.; Ramireddy, C.; Tuzar, Z.; Webber, S. E. *Macromolecules* **1991**, *24*, 6300.
(5) Kiserow, D.; Procházka, K.; Ramireddy, C.; Tuzar, Z.; Munk, P.; Webber, S. E. *Macromolecules* **1992**, *25*, 461.
(6) Tian, M.; Arca, E.; Tuzar, Z.; Webber, S. E.; Munk, P. *J. Polym. Sci., Polym. Phys.* **1995**, 1713.
(7) Tian, M. *Ph.D. Thesis*, University of Texas at Austin, 1994.
(8) Seidell, A. *Solubilities of Organic Compounds*; Van Nostrand Co.: New York, 1941.
(9) Barton, A. F. M. *CRC Handbook of Polymer-Liquid Interaction Parameters and Solubility Parameters*; CRC Press: Ann Arbor, MI, 1990.
(10) Brandrup, J.; Immergut, E. H. *Polymer Handbook*, 3rd ed.; J. Wiley: New York, 1989.
(11) *Handbook of Chemistry and Physics*, 76th ed.; Lide, David R., Ed.; CRC Press: Boca Raton, FL, 1996.

MA961701C